



2007

## Electron Trapping in a One-Dimensional Semiconductor Quantum Wire with Multiple Impurities

S. Tanaka

S. Garmon

Gonzalo Ordonez

Butler University, [gordonez@butler.edu](mailto:gordonez@butler.edu)

T. Petrosky

Follow this and additional works at: [https://digitalcommons.butler.edu/facsch\\_papers](https://digitalcommons.butler.edu/facsch_papers)



Part of the [Quantum Physics Commons](#)

---

### Recommended Citation

Tanaka, S.; Garmon, S.; Ordonez, Gonzalo; and Petrosky, T., "Electron Trapping in a One-Dimensional Semiconductor Quantum Wire with Multiple Impurities" *Physical Review B* / (2007): -. Available at [https://digitalcommons.butler.edu/facsch\\_papers/722](https://digitalcommons.butler.edu/facsch_papers/722)

This Article is brought to you for free and open access by the College of Liberal Arts & Sciences at Digital Commons @ Butler University. It has been accepted for inclusion in Scholarship and Professional Work - LAS by an authorized administrator of Digital Commons @ Butler University. For more information, please contact [digitalscholarship@butler.edu](mailto:digitalscholarship@butler.edu).

# Electron trapping in a one-dimensional semiconductor quantum wire with multiple impurities

S. Tanaka,<sup>1</sup> S. Garmon,<sup>2</sup> G. Ordóñez,<sup>3</sup> and T. Petrosky<sup>2,\*</sup>

<sup>1</sup>Department of Physical Science, Osaka Prefecture University, Sakai 599-8531, Japan

<sup>2</sup>Center for Complex Quantum Systems, The University of Texas at Austin, Austin, Texas 78712, USA

<sup>3</sup>Physics and Astronomy Department, Butler University, 4600 Sunset Avenue, Indianapolis, Indiana 46208, USA

(Received 7 September 2007; published 19 October 2007)

We demonstrate the trapping of a conduction electron between two identical adatom impurities in a one-dimensional semiconductor quantum-dot array system (quantum wire). Bound steady states arise even when the energy of the adatom impurity is located in the continuous one-dimensional energy miniband. The steady state is a realization of the bound state in continuum (BIC) phenomenon first proposed by von Neuman and Wigner [Phys. Z. **30**, 465 (1929)]. We analytically solve the dispersion equation for this localized state, which enables us to reveal the mechanism of the BIC. The appearance of the BIC state is attributed to the quantum interference between the impurities. The Van Hove singularity causes another type of bound state to form above and below the band edges, which may coexist with the BIC.

DOI: 10.1103/PhysRevB.76.153308

PACS number(s): 73.20.Hb, 73.21.Cd, 73.21.Fg, 78.67.Lt

One-dimensional semiconductor quantum wires (1D-QWRs) have been extensively investigated theoretically and experimentally over the past two decades.<sup>1-3</sup> Thanks to advances in nanotechnology, various ways to manufacture semiconductor 1D-QWR have been developed.<sup>4</sup> The quantum confinement of electrons in these structures greatly modifies the density of states of carriers resulting in completely different electronic and optical properties from the bulk system.<sup>1-4</sup> The 1D-QWR has also been fabricated in metallic systems and organic molecular systems.<sup>5,6</sup>

In a previous report,<sup>7</sup> we presented the charge transfer from an adatom localized state to the 1D conduction miniband associated with a quantum wire or quantum-dot array. Due to a singularity in the density of electron states at either edge of the electronic miniband, there is a nonanalytic  $g^{4/3}$  enhancement of the charge transfer rate when the adatom energy is near the band edges, where  $g$  is the dimensionless coupling constant describing the hybridization interaction between the adatom localized state and the miniband. We also presented Fano's absorption spectrum attributed to the transition of an electron from a core level of the adatom to the conduction miniband, with which we were able to explicitly separate the irreversible Markovian exponential decay and the reversible non-Markovian power law decay contributions to the time evolution of the system.

Here, we shall report a different phenomenon: electron trapping between two identical adatoms in the 1D miniband due to quantum interference. The physical situation we consider in this Brief Report is depicted in Fig. 1(a). We find that a bound steady state appears even when the energy of the adatom impurity energy is located in the 1D miniband such that an electron is trapped between the two identical adatoms. The steady state is an example of "bound states in continuum" (BIC) first proposed by Von Neumann and Wigner<sup>8</sup> for oscillating attractive potentials. Since then, a number of theoretical studies of BIC have been reported.<sup>9,10</sup> Experimental evidence of BIC has also been reported in positive energy bound states in superlattice structures of quantum wells with a single impurity site<sup>11</sup> or in a single defect stub.<sup>12</sup> In a recent article, one of the authors presented another example of BIC in a double-cavity (or double-dot), two-dimensional electron waveguide.<sup>10</sup> In this Brief Report,

we shall present this interesting feature of BIC in a 1D-QWR with multiple impurities, which is physically quite different from the waveguide.

We consider a 1D-QWR consisting of  $N+1$  quantum dots, where we consider a single bound state for each quantum dot, as shown in Fig. 1(b). An electron can tunnel between these bound states through the transfer integral  $-B/2$ , which leads to the formation of the continuous 1D miniband along the wire with the width  $B$  in the limit  $N \rightarrow \infty$ .<sup>1-3</sup> In the present work, we assume that the lateral extent perpendicular to the wire axis is small such that the quantum confinement in a given quantum dot is so strong that the energy separation between the lowest bound state and the first excited bound state in that dot is far larger than the 1D miniband width. Therefore, we can consider electron transport along the chain without causing any excitation perpendicular to it.

In addition, the adatom states with energy  $E_0$  are located at the  $n$ th and  $(-n)$ th sites; they are hybridized with the bound states within these dots with the coupling strength  $g$  because the size of the quantum dot, which usually ranges

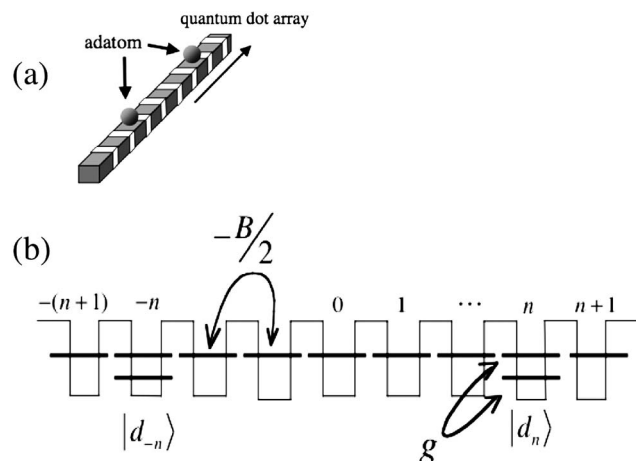


FIG. 1. (a) Two identical adatoms attached to a 1D quantum-dot array and (b) level structures of the adatom localized states and the bound states in each quantum dot. The adatoms are located at the  $n$ th and  $(-n)$ th dots.

from several to hundreds of nanometers, is far larger than the size of the adsorbates. We shall simply refer to the adatom localized states as the impurity states. We represent this single electron system by the tight binding Hamiltonian including the two impurity states hybridized with the miniband as

$$H = E_0(d_{-n}^+d_{-n} + d_n^+d_n) - \frac{B}{2} \sum_{\langle l,l' \rangle} \tilde{a}_l^+ \tilde{a}_{l'} + gB \sum_{l=-n,n} (d_l^+ \tilde{a}_l + \tilde{a}_l^+ d_l), \quad (1)$$

where  $d_{-n}$  and  $d_n$  are the fermionic annihilation operators for the electron in the impurity states,  $\tilde{a}_l$  is the fermionic operator representing the bound state in the  $l$ th quantum dot, and the symbol  $\langle l,l' \rangle$  represents the sum over nearest neighbors. We introduce the wave number representation  $a_k = \sum_{l=-N/2}^{N/2} \tilde{a}_l e^{ikl} / \sqrt{N+1}$  and impose the usual periodic boundary conditions on the 1D-QWR that will result in a continuous energy spectrum for the miniband in the limit  $N \rightarrow \infty$ . For finite  $N$ , we have a discrete wave number with  $k_j = 2\pi j / (N+1)$ , where  $j$  is an integer that runs from  $-N/2$  to  $N/2$ . The Hamiltonian  $H$  is then cast into

$$H = E_0(d_{-n}^+d_{-n} + d_n^+d_n) + \sum_{j=-N/2}^{N/2} E_{k_j} a_{k_j}^+ a_{k_j} + \frac{gB}{\sqrt{N}} \sum_{\alpha=-n,n} \sum_{j=-N/2}^{N/2} (d_\alpha^+ a_{k_j} e^{ik_j \alpha} + a_{k_j}^+ d_\alpha e^{-ik_j \alpha}), \quad (2)$$

where  $E_k = -B \cos k$  is the energy dispersion of the miniband, which leads to the density of states  $\rho(E_k) \equiv \frac{1}{\pi} (B^2 - E_k^2)^{-1/2}$  with singularities at both edges of the miniband,  $E_k = \pm B$ . One advantage of 1D-QWR is that one can change the value of  $B$  by changing the potential barriers between the quantum dots using precise nanotechnology<sup>1,2</sup>: the value of  $B$  is estimated to be about  $\sim 140$  meV for GaAs/AlGaAs QWR when the adjacent distance of the quantum dots is  $\sim 25$  nm.<sup>1</sup> The parameter  $gB$  is the coupling constant representing the charge transfer between the adatom and the semiconductor surface, and it has been estimated to be less than 70 meV for physisorbed molecules on the semiconductor surface.<sup>13</sup>

The Hamiltonian may be decoupled by introducing symmetric ( $s$  state) and antisymmetric states ( $p$  state) both for the impurity states and the 1D miniband (with mode  $k$ ) through  $s \equiv (d_n + d_{-n}) / \sqrt{2}$ ,  $p \equiv (d_n - d_{-n}) / \sqrt{2}$ ,  $S_k \equiv (a_k + a_{-k}) / \sqrt{2}$ , and  $P_k \equiv (a_k - a_{-k}) / \sqrt{2}$ . We then have  $H = H_s + H_p$ , where

$$H_s = E_0 s^+ s + \sum_{j=0}^{N/2} E_{k_j} S_{k_j}^+ S_{k_j} + \frac{2gB}{\sqrt{N}} \sum_{j=0}^{N/2} [s^+ S_{k_j} \cos(k_j n) + \text{H.c.}], \quad (3a)$$

$$H_p = E_0 p^+ p + \sum_{j=0}^{N/2} E_{k_j} P_{k_j}^+ P_{k_j} + \frac{2igB}{\sqrt{N}} \sum_{j=0}^{N/2} [p^+ P_{k_j} \sin(k_j n) - \text{H.c.}], \quad (3b)$$

where H.c. stands for Hermitian conjugate. Both  $H_s$  and  $H_p$  take the form of the Friedrichs-Fano (Newns-Anderson)

Hamiltonian,<sup>16-19</sup> which has been used extensively to describe the electronic states of adsorbates on metal and semiconductor surfaces.<sup>20</sup> These bilinear Hamiltonians can be diagonalized by a linear transformation.<sup>7,16</sup> However, we do not need the explicit form of the transformation for our purposes in this Brief Report.

The self-energies for the  $s$  and  $p$  symmetrized impurity states are given in the limit  $N \rightarrow \infty$  by

$$\begin{aligned} \Xi^{s,p}(z) &= \frac{g^2 B^2}{2\pi} \int_{-\pi}^{\pi} dk \frac{1 \pm \cos(2kn)}{z + B \cos k} \\ &= \frac{g^2 B}{\sqrt{\xi^2 - 1}} [1 \pm (-\xi + \sqrt{\xi^2 - 1})^{2n}] \\ &= \frac{g^2 B}{i \sin \theta} (1 \pm e^{i2n\theta}), \end{aligned} \quad (4)$$

where we have put  $\xi \equiv z/B = -\cos \theta$ . In Eq. (4), the  $+$  sign is for the  $s$  state while the  $-$  sign is for the  $p$  state. Care must be taken when choosing the appropriate branch for the analytic continuation of  $\sqrt{\xi^2 - 1}$  so that the localized state will decay toward the future.<sup>21</sup>

The solutions of the dispersion equation for the  $s$  and  $p$  symmetrized states,

$$\eta^{s,p}(z) \equiv z - E_0 - \Xi^{s,p}(z) = 0, \quad (5)$$

consist of the pole in the lower-half complex plane in the second Riemann sheet corresponding to the unstable decaying state and the poles on the real axis of the first sheet corresponding to the stable states.

It is found from Eq. (4) that as  $z$  moves on the real axis from  $-B$  to  $B$ , the self-energies for the  $s$  and  $p$  states periodically vanish as  $\exp[i2n\theta_m] = \mp 1$  ( $-$  and  $+$  signs are for the  $s$  and  $p$  states, respectively) at  $z = E_m$ , where  $E_m = -B \cos(m\pi/2n) \equiv -B \cos(\theta_m)$ , with  $m = 1, 3, \dots, 2n-1$  for the  $s$  state and  $m = 2, 4, \dots, 2n-2$  for the  $p$  state. As an illustration, we show the real part and imaginary part of  $\Xi^p(E)$  for the  $p$  states in Fig. 2 for the case of  $n=4$ , where the horizontal axis stands for  $E/B$ . As shown,  $\text{Re } \Xi^p(E) = \text{Im } \Xi^p(E) = 0$  at  $\theta_m = 2\pi/8, 4\pi/8$ , and  $6\pi/8$ . The real and imaginary parts of  $\Xi^s(E)$  for the  $s$  states are also shown in Fig. 3 for the case of  $n=4$ . In this case, for  $\theta_m = \pi/8, 3\pi/8, 5\pi/8$ , and  $7\pi/8$ ,  $\text{Re } \Xi^s(E) = \text{Im } \Xi^s(E) = 0$ . It should be emphasized that the values of  $E_m$  do not depend on the coupling constant  $g$ , that is, the position of  $E_m$  is exclusively determined by the energy level structures of the 1D miniband as will be shown below.

The solution of the dispersion equation [Eq. (5)] is determined by the intersection of  $E - E_0$  and  $\Xi(E)$  as a function of  $E$ . Therefore, when  $E_0 = E_m$ ,  $z = E_0$  is a stable solution of the dispersion equation in the 1D miniband; this gives a BIC state which never decays even though the energy  $E_0$  is located in the 1D miniband, irrespective of the coupling constant  $g$ . The number of such solutions  $E_m$  increases as the separation between the impurity sites  $2n$  increases:  $n-1$  is the number of solutions for the  $p$  state and  $n$  for the  $s$  state.

We shall now show that in the BIC states, the electron is completely trapped between the two impurity sites. We con-

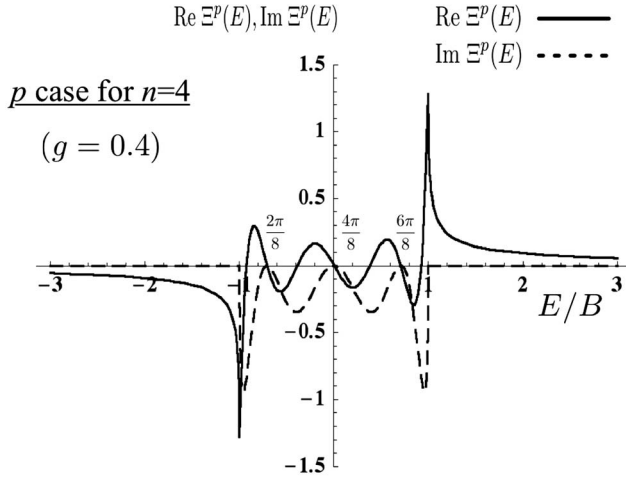


FIG. 2. The real part  $\text{Re } \Xi^p(E)$  and the imaginary part  $\text{Im } \Xi^p(E)$  of the self-energy of the  $p$  state for  $n=4$  as a function of real  $E$ , where the horizontal axis stands for  $E/B$ . Inside the miniband  $E/B=-1$  to  $E/B=1$ , there are three points of  $E_m$  where  $\Xi(E_m)=0$ . In the figure, we indicate the value of  $\theta_m$  corresponding to the  $E_m$ 's. No divergence in  $\Xi^p(E)$  occurs at the band edges.

consider the  $s$  symmetry case (the  $p$  symmetry case can be demonstrated in a similar manner). In terms of the site representation, the symmetrized basis is given by  $|\tilde{S}_0\rangle = |\tilde{a}_0\rangle$  and  $|\tilde{S}_l\rangle = (|\tilde{a}_l\rangle + |\tilde{a}_{-l}\rangle)/\sqrt{2}$  for  $l=1, 2, \dots$ , where  $|\tilde{a}_n\rangle \equiv \tilde{a}_n^+|0\rangle$ , etc., with  $|0\rangle$  the electron vacuum state. In terms of this basis,  $H_s$  is rewritten as  $H_s = H_{in} + H_{out}$ , where

$$H_{in} = E_0|s\rangle\langle s| + \sum_{l=0}^{n-1} v_l(|\tilde{S}_l\rangle\langle\tilde{S}_{l+1}| + \text{H.c.}) + gB(|s\rangle\langle\tilde{S}_n| + \text{H.c.}), \quad (6a)$$

$$H_{out} = \sum_{l=n}^{\infty} v_l(|\tilde{S}_l\rangle\langle\tilde{S}_{l+1}| + \text{H.c.}). \quad (6b)$$

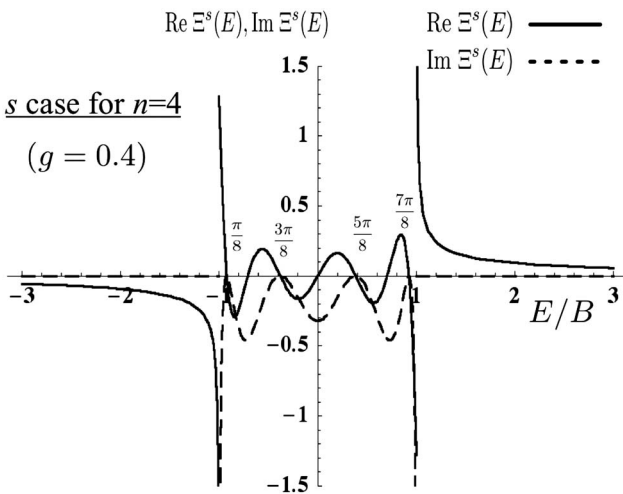


FIG. 3. The same plot of the  $s$  state for  $n=4$  as in Fig. 2. Inside the 1D miniband, there are four points of  $E_m$  where  $\Xi(E_m)=0$ . The value of  $\theta_m$  corresponding to the points of  $E_m$  are indicated.  $\text{Re } \Xi^s(E)$  diverges at  $E/B = \pm 1$ , while  $\text{Im } \Xi^s(E)$  does not.

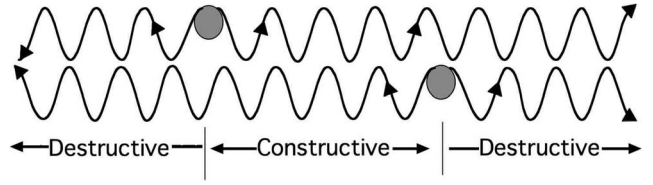


FIG. 4. Schematic picture of the quantum interference in BIC. The spontaneously decaying waves constructively interfere with each other between the impurities, while they destructively interfere outside the impurities.

In Eqs. (6a) and (6b),  $v_0 = -B/\sqrt{2}$  and  $v_l = -B/2$  for  $l=1, 2, \dots$ . Let us first consider the eigenvalue problem of  $H_{in}$  instead of  $H_s$ :  $H_{in}|\phi_\lambda^{in}\rangle = \tilde{E}_\lambda^{in}|\phi_\lambda^{in}\rangle$ . For the eigenstate of  $H_{in}$ , it can be proven that

$$\tilde{E}_\lambda^{in} - E_0 = gB \frac{\langle \tilde{S}_n | \phi_\lambda^{in} \rangle}{\langle s | \phi_\lambda^{in} \rangle}. \quad (7)$$

It follows from Eq. (7) that if  $\tilde{E}_\lambda^{in} = E_0$  (as we have discussed in the case for the BIC), the eigenstate does not involve the  $|\tilde{S}_n\rangle$  component, i.e.,  $|\phi_\lambda^{in}\rangle = (|s\rangle\langle s| + \sum_{l=0}^{n-1} |\tilde{S}_l\rangle\langle\tilde{S}_l|) |\phi_\lambda^{in}\rangle$ . As a result, the state  $|\phi_\lambda^{in}\rangle$  does not couple with the outer states of  $|\tilde{S}_l\rangle$  ( $l=n+1, n+2, \dots$ ) through  $H_{out}$ . That is, it is completely localized within the two impurities; it is also an eigenstate of the total Hamiltonian  $H_s$ :  $H_s|\phi_\lambda^{in}\rangle = \tilde{E}_\lambda^{in}|\phi_\lambda^{in}\rangle$  with  $\tilde{E}_\lambda^{in} = E_0$ .

We show the explicit form of the eigenstates for some cases: the BIC for the  $n=1$ ,  $s$  case is written as  $|\psi^{1,s}\rangle = (|s\rangle + \sqrt{2}g|\tilde{S}_0\rangle)/\sqrt{1+2g^2}$ , with  $H_s|\psi^{1,s}\rangle = 0$ , and for the  $n=2$ ,  $p$  case  $|\psi^{2,p}\rangle = (|p\rangle + 2g|\tilde{P}_0\rangle)/\sqrt{1+4g^2}$ , with  $H_p|\psi^{2,p}\rangle = 0$ . For the  $n=2$ ,  $s$  case, they are represented by  $|\psi_\pm^{2,s}\rangle = (|s\rangle + 2g(|\tilde{S}_1\rangle \pm |\tilde{S}_0\rangle))/\sqrt{1+8g^2}$ , with  $H_s|\psi_\pm^{2,s}\rangle = \pm|\psi_\pm^{2,s}\rangle/\sqrt{2}$ . On the other hand, the eigenstates of  $H_s$  with eigenvalues different from  $E_0$  necessarily involve the  $|\tilde{S}_n\rangle$  components, such that those states couple with the outer states and are therefore delocalized. This is consistent with the ordinary observation that the continuum under most circumstances has a destabilizing effect. However, below, we will discuss an exception which results in a different kind of bound state, even though  $\tilde{E}_\lambda^{in} = E_0$  is not satisfied.

The mechanism by which these steady states occur inside the continuous energy spectrum may be understood as follows. Suppose that an electron is localized at one of the two impurity states. Due to the resonance interaction with the 1D miniband, the impurity state decays spontaneously into the 1D miniband emitting an electron wave, as shown in Fig. 4. When the free electron wave reaches the other impurity, the electron transitions into the other localized impurity state. This impurity state also decays into the 1D miniband due to the resonance interaction, just as the first site. The emitted free propagating electron wave thus goes back and forth between the impurity sites, just like a ping-pong game.<sup>14</sup> Our results show that one can practically manufacture such a semiconductor 1D-QWR with double impurities that the

electron waves emitted from the impurities constructively interfere with each other inside the two impurities, while they destructively interfere outside the impurities, as schematically illustrated in Fig. 4. As a result of quantum interference, the BIC is localized between the two impurities.

As for the  $s$  state, two stable states always appear just below and above the 1D miniband due to the divergence of the density of states at the band edges.<sup>7,15</sup> The wave function of this state outside the miniband is largely extended to states representing sites outside the impurities, contrary to the BIC. Despite being coupled to the outer sites, this state remains stable, as mentioned above. It is interesting that different types of steady states coexist when the BIC appears. For the  $p$  symmetry, however, the factor of  $\sin(kn)$  in the hybridization term in Eq. (3b) suppresses the divergence of the density

of states, such that the stable state outside the miniband does not appear when  $E_0$  is located inside the miniband.

These BIC states in the 1D-QWR may be experimentally observed with the use of the optical absorption spectrum as we discussed in Ref. 7. We hope to challenge the experimentalist to observe this interesting phenomena through the absorption spectrum or by other means.

We thank W. Schieve, G. Sudarshan, L. E. Reichl, N. Hatano, and H. Nakamura for insightful discussions. This material is based upon work supported by the National Science Foundation under Grant No. 0611506. This work was supported by the Grant-in-Aid for Scientific Research from the Ministry of Education, Science, Sports, and Culture of Japan.

---

\*petrosky@physics.utexas.edu

<sup>1</sup>S. E. Ulloa, E. Castano, and G. Kirczenow, Phys. Rev. B **41**, 12350 (1990).

<sup>2</sup>L. P. Kouwenhoven, F. W. J. Hekking, B. J. van Wees, C. J. P. M. Harmans, C. E. Timmering, and C. T. Foxon, Phys. Rev. Lett. **65**, 361 (1990).

<sup>3</sup>A. Richter G. Behme, M. Suptitz, C. Lienau, T. Elsaesser, M. Ramsteiner, R. Notzel, and K. H. Ploog, Phys. Rev. Lett. **79**, 2145 (1997).

<sup>4</sup>R. Nötzel and K. H. Ploog, Adv. Mater. (Weinheim, Ger.) **5**, 22 (1993); X.-L. Wang and V. Voliotis, J. Appl. Phys. **99**, 121301 (2006).

<sup>5</sup>I. Barke *et al.*, Solid State Commun. **142**, 617 (2007).

<sup>6</sup>C. Joachim, J. K. Gimzewski, and A. Aviram, Nature (London) **408**, 541 (2000).

<sup>7</sup>S. Tanaka, S. Garmon, and T. Petrosky, Phys. Rev. B **73**, 115340 (2006).

<sup>8</sup>J. von Neumann and E. Wigner, Phys. Z. **30**, 465 (1929).

<sup>9</sup>F. H. Stillinger and D. R. Herrick, Phys. Rev. A **11**, 446 (1975); L. Fonda and R. G. Newton, Ann. Phys. (N.Y.) **10**, 490 (1960);

W. Vanroose, Phys. Rev. A **64**, 062708 (2001); K.-K. Voo and C. S. Chu, Phys. Rev. B **74**, 155306 (2006); S. Longhi, Eur. Phys. J. B **57**, 45 (2007).

<sup>10</sup>G. Ordóñez, K. Na, and S. Kim, Phys. Rev. A **73**, 022113 (2006).

<sup>11</sup>F. Capasso, C. Sirtori, J. Faist, D. L. Sivco, S.-N. G. Chu, and A. Y. Cho, Nature (London) **358**, 565 (1992).

<sup>12</sup>P. S. Deo and A. M. Jayannavar, Phys. Rev. B **50**, 11629 (1994).

<sup>13</sup>O. Björneholm, A. Nilsson, A. Sandell, B. Hermnäs, and N. Mårtensson, Phys. Rev. Lett. **68**, 1892 (1992).

<sup>14</sup>G. Ordóñez and S. Kim, Phys. Rev. A **70**, 032702 (2004).

<sup>15</sup>T. Petrosky, C.-O. Ting, and S. Garmon, Phys. Rev. Lett. **94**, 043601 (2005).

<sup>16</sup>K. Friedrichs, Commun. Pure Appl. Math. **1**, 361 (1948).

<sup>17</sup>E. C. G. Sudarshan, *1962 Brandeis Lectures in Physics* (Benjamin, New York, 1962).

<sup>18</sup>U. Fano, Phys. Rev. **124**, 1866 (1961).

<sup>19</sup>P. W. Anderson, Phys. Rev. **124**, 41 (1961).

<sup>20</sup>G. P. Brivio and M. I. Trioni, Rev. Mod. Phys. **71**, 231 (1999).

<sup>21</sup>T. Petrosky, S. Tasaki, and I. Prigogine, Physica A **173**, 175 (1991).